Journal of
Materials Chemistry C

Materials for optical, magnetic and electronic devices

Accepted Manuscript

This article can be cited before page numbers have been issued, to do this please use: K. Feng, L. Xu, Y. Xiong, L. Sun, H. Yu, M. Wu, A. A. Thant and B. Hu, *J. Mater. Chem. C*, 2020, DOI: 10.1039/C9TC06277G.

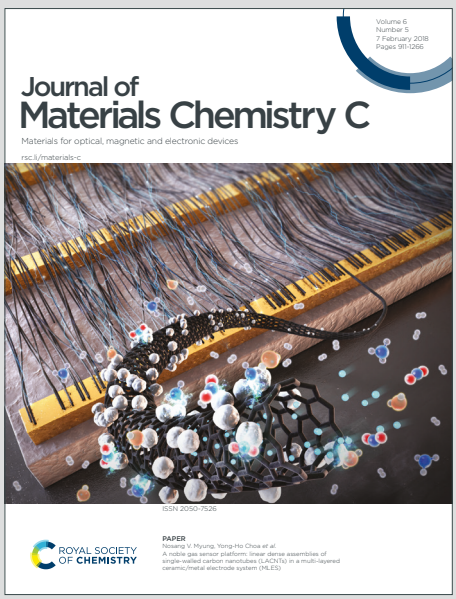

ROYAL SOCIETY OF CHEMISTRY

rsc.li/materials-c

PEDOT:PSS and Ni-based Thermoelectric Generator for Solar Thermal Energy Conversion

Kai Feng [a], Ling Xu [a, *], Yan Xiong [a], Lin Sun [a], Huayang Yu [a], Mengying Wu [a], Aye Aye Thant [b], Bin Hu [a, c,*]

[a] *Wuhan National Laboratory for Optoelectronics, China-EU Institute for Clean and Renewable Energy, Huazhong University of Science and Technology, Wuhan 430074, China.*

[b] *Department of Physics, University of Yangon, Kamaryut, Yangon, 11041, Myanmar.*

[c] *Department of Materials Science and Engineering, University of Tennessee, Knoxville, TN 37996, USA.*

* Corresponding Author, E-mail: xuling@mail.hust.edu.cn (L.Xu), bhu@utk.edu (B. Hu)

Kai Feng, Dr. Ling Xu , Yan Xiong , Lin Sun , Huayang Yu , Mengying Wu, Prof. Bin Hu
Wuhan National Laboratory for Optoelectronics, China-EU Institute for Clean and Renewable Energy,
Huazhong University of Science and Technology,
Wuhan 430074, China.

Prof. Aye Aye Thant
Department of Physics,
University of Yangon, Kamaryut,
Yangon, 11041, Myanmar.

Prof. Bin Hu
Department of Materials Science and Engineering,
University of Tennessee,
Knoxville, TN 37996, USA.

View Article Online
DOI: 10.1039/C9TC06277G

Abstract:

Searching an inexpensive and effective way to improve the thermoelectric properties of organic materials can greatly expand the practical application of thermoelectric thin film generator. Here, we adopt the triple treatment of ethylene glycol ($(CH_2OH)_2$) , ethanol(C_2H_5OH) doping and $(CH_2OH)_2$ dedoping to tune the micro stacking structure of PEDOT:PSS. The obtained PEDOT:PSS thermoelectric film material has the highest power factor (PF) up to 330.597 μWm^{-1},which stems from the high Seebeck coefficient (S) and conductivity (σ). Furthermore, we fabricated the thermoelectric generator to explore the conversion process of the solar energy photothermal. The maximum power output of the home-made module device with solar energy as the heat source reaches 9.8 nW. This work is a prospective experiment for development of the solar photothermal conversion based on the thin film and device.

Key words:

PEDOT:PSS, Nickel, Photothermal conversion efficiency, Seebeck coefficient, Electrical conductivity

View Article Online
DOI: 10.1039/C9TC06277G

1. Introduction

Solar energy is a kind of clean, efficient and abundant energy, one of the main approaches to utilize solar energy is converted to electric energy [1]. Basically, the utilization of solar energy is still very rare at present. Its utilization mainly applied in photovoltaics through monocrystalline and polycrystalline silicon solar cells which owns the power conversion efficiency (PCE) close to 25.2%, but the utilization of solar energy in thermoelectric field is very limited. The photovoltaic devices often use visible sunlight [2]. While, thermoelectric devices need heat source from infrared sunlight. We know that visible light (380-760 nm) accounts for 45% of the total solar energy, and infrared light (800-3000 nm) accounts for 42% of the total solar energy [3]. If the utilization of solar energy can be expanded from visible light area to infrared area through thermoelectric devices, the conversion efficiency of solar-to-electric energy will be greatly improved. In addition, In the process of photoelectric conversion, the efficiency of solar cell is directly affected by the intensity of solar radiation or other environmental changes. Fortunately, the productivity of thermoelectric generator would not be seriously affected by the weather, location and other conditions [4].

Thermoelectric conversion of solar energy requires the functional materials with thermoelectric conversion effect. Generally, these thermoelectric materials are evaluated by thermoelectric merit value ZT. $ZT=S^2\sigma/\kappa$, where S， σ， κ are Seebeck coefficient, electrical conductivity and thermal conductivity, respectively [5]. Excellent thermoelectric materials require high conductivity and Seebeck coefficient, as well as low thermal conductivity. Nowadays, inorganic thermoelectric materials have high conductivity and Seebeck coefficient but immense thermal conductivity; while organic thermoelectric materials have low thermal conductivity, but their electrical conductivity are depressed. In general, the thermoelectric materials possessing high electrical conductivity and Seebck coefficient and low thermal conductivity simultaneously are very demanding. Selecting conductive organic materials is an effective way to achieve high power factor PF ($PF=S^2\sigma$) [6-7]. Organic conductive materials have

View Article Online
DOI: 10.1039/C9TC06277G

attracted more and more attention in the field of thermoelectricity due to the printable, flexible characteristics [8]. Among these, PEDOT: PSS [9], PPy [10], MEH-PPV [11] are the organic thermoelectric materials with high thermal power factor, the thermal stability of PEDOT is the most widely studied. To be honest, commercial PEDOT: PSS thermoelectric property is not satisfacted due to its inherent low electronic conductivity. There are several ways to improve the thermoelectric properties of PEDOT:PSS (S and σ). For example: (1) Pretreatment of PEDOT: PSS by doping high boiling point organic solvents (Dimethyl sulfoxide), (2) High dielectric constant solvents (concentrated sulfuric acid, salt solution) [12-13].These ways can increase the density of states of organic molecules [14], promote the separation of PEDOT from PSS [15], modify carrier transport path to optimize thermoelectric properties [16]. However, approaches of this kind carry with them various well known limitations, and the films with high ZT value (the maximum value is about 0.42) are usually prepared by spin coating, which is not suitable for large-scale fabrication

Notably, Aiming at solar energy photothermal utilization, countries around the world are conducting this research, the purpose is to collect more solar energy form artificial high-temperature parts, and improve the thermal factor diffusion. Chen et al reported that they had developed planar solar thermal devices which could generate 14.6% of the electricity [17], and they advocated that the use of solar spectral absorption devices and nanostructures of new concepts of thermal elements can improve the efficiency of devices. On the other hand, Baranowski and others advocated that the theoretical conversion efficiency of 30.6% can be achieved at 1500 °C by using the analytic heat of solar energy concentration and the element with ZT value of 2 [18]. In this case, because the working environment is up to 1500 °C, it is necessary to design a solar collector that can form this high temperature and maintain high temperature thermal work condition. At the same time, it is necessary to develop thermoelectric components that can produce the best ZT value of power generation efficiency at high temperature [19]. Lately, Olsen of the National Renewable Energy Laboratory explained the design and fabrication of efficient thermoelectric devices consisting of solar collectors and thermal elements, and explained the thermal power generation and life of

View Article Online
DOI: 10.1039/C9TC06277G

thermoelectric devices when measuring the economic effect of power generation [20] . Han Shengyou of Korea Institute of Machinery used solar energy collector thermal elements to test its performance, and concentrated on solar energy balloons to generate power for thermoelectric modules [21]. he obtained about 0.74 watts of power output at 50 ^{o}C [22]. The above research mainly focuses on the high temperature research of solar energy concentrating, there are few studies on the photothermal utilization of non-concentrating low temperature and room temperature solar energy.

Herein, we adopt PEDOT:PSS modified by $(CH_2OH)_2$ doping, C_2H_5OH doping, $(CH_2OH)_2$ immersion triple treatment process, which enhance the electrical conductivity and Seebeck coefficient greatly. In addition to the high integrated absorptivity (α) of solar spectrum and low emissivity (ε) of infrared, an excellent thermoelectric material can also be produced on a large scale with low cost, theoretically, Ni is a promising n-type metallic thermoelectric material for its high electrical conductivity and excellent Seebeck coefficient. With these aims in view, we have developed a process, for the deposition of Nickle (Ni) metal, Ni possesses a high electrical conductivity and an excellent Seebeck coefficient among metals. Because the thin film characteristics, the temperature difference is not large in the thin film device. There is less application and research of photothermal for the thin film thermoelectric device. On the other hand, the characteristics of the films are flexible and bendable, and easy to produce in large areas. They are one of a class of materials that have great application prospects. We found that although the films have small temperature differences, they have a large temperature gradient field, the temperature gradient field can produce a large polarization filed, the temperature gradient polarization effect further enhances the performance of thermoelectric thin film devices. Therefore, a homemade organic-inorganic thermoelectric generator which is composed of optimized PEDOT: PSS as P-legs and Ni as N-legs, the generator using solar radiation as a heating source exhibits a potential power output of 9.8 nW.

2. Experimental section

View Article Online
DOI: 10.1039/C9TC06277G

2.1 Chemicals and materials

PEDOT: PSS (M122 PH1000, in the ratio 1.0-1.3%) is purchased from Clevios Company. $(CH_2OH)_2$ and C_2H_5OH (purity 99%) are purchased from China Pharmaceutical Company. Ni evaporator (purity 99.99%) is purchased from Beijing Zhongjin Research Corporation. All chemicals are used as received without further purification.

2.2 Sample preparation

$(CH_2OH)_2$ and C_2H_5OH are doped in PEDOT:PSS precursor solution in sequence to improve the thermoelectric properties of PEDOT: PSS films. In details, $(CH_2OH)_2$ is firstly added into 1 ml PH1000 .Then, the mixture is stirred for 24h. After that, 3 ml C_2H_5OH and deionized water with a volume ratio of 1:2 are added to 1ml mixture obtained in the previous step of the above solution. Then the mixture is sonicated for 2 h. Then, it is drop casted on a glass substrate which is pretreated by sonication in detergent, acetone, and isopropyl alcohol, respectively. The film is then annealed on a hot plate at 65 ° C for 30 mins. In the following step, the annealed film is immersed in $(CH_2OH)_2$ for 100 mins and washed with deionized water to remove any residual of $(CH_2OH)_2$. The films are finally dried with N_2 flow before further measurements. PEDOT:PSS film with 1.45 μm thickness is obtained, the PEDOT:PSS molecular structure showed in Figure 1(a).

2.3 Device preparation

Different volume fractions of $(CH_2OH)_2$ and C_2H_5OH are added into milliliter of PEDOT: PSS respectively. the solution is spread on a clean large area glass substrate, annealed in air at 65 ℃ for 3h, then crystallized into thin film. The thin film is treated with glycol to obtain self-supporting flexible film. In order to explore the application of thermoelectric generator in the field of photothermal, the above self-supporting thin film is transferred to the glass substrate. p-leg with a specification of 2.5 cm x 0.3 cm x 1.5 μ m is fabricated. The Ni equivalent to p-leg is evaporated and plated with n-leg (2.5 cm x 0.3 cm x 150 nm), and silver paste is selected as the connecting agent in

View Article Online
DOI: 10.1039/C9TC06277G

the circuit. The device structure is shown on the Figure 1(b).

2.4 Characterizations and Measurements

In order to minimize the experimental uncertainties under direct sun light, a solar simulator (Newport Co. Oriel Xenon Arc lamp) is used as the light source. The performance parameters of the solar simulator are based on the ASTM standard (ASTM G-173, 2011), including spectral match (fraction of ideal percentage) of 0.7-1.25, non-uniformity of irradiance up to 5% and temporal instability up to 5%. Seebeck coefficient measurement is carried out on a homemade set-up consisting of a ceramic wafer heating stage, voltage and temperature controlling system. Conductivity, carrier density and mobility of the films are calculated by measuring Hall Effect on ECOPIA HMS-5500. UV-visible spectra is recorded on uv-3600, Shimadzu, Japan. Film morphology is characterized by atomic force microscopy (AFM Bruker Company). Paramagnetic signal is obtained through the electron paramagnetic resonance (EPR, Bruker A300)

3. Results and Discussions

3.1 Thermoelectric Properties of treated PEDOT:PSS

Figure 2 (a) shows the thermoelectric characteristics of different PEDOT:PSS films under ambient conditions. The electrical conductivities of original PEDOT:PSS, PEDOT:PSS mixed with $(CH_2OH)_2$ (PEDOT-EG), PEDOT:PSS mixed with alcohol and EG (PEDOT:PSS-EG and etOH) are 4.27 S/cm, 43.3 S/cm and 890.7 S/cm, respectively. After the treatment of immersing the PEDOT:PSS-etOH and EG film into EG, the electrical conductivity is enhanced to 1478.577 S/cm. Simultaneously, the Seebeck coefficient of the original thermoelectric films increase from 12.74 μV/K to 33.52 μV/K, 40.29 μV/K, and 47.16 μV/K. Correspondingly, the PF are calculated to 0.069, 61.037, 144.586, and 330.597 μWm^{-1}, respectively. This is suggested to be induced by phase separation between PEDOT chains and PSS after EG, the acting force substantially reduce between PEDOT and PSS molecular chain, making the non-conducting polyanion PSS molecular chain to partially dedoping, thus

View Article Online
DOI: 10.1039/C9TC06277G

increasing the electrical conductivity of PEDOT:PSS, etOH addition and post-treatment with EG, which will be demonstrated in details in the following parts. Figure 2 (b) shows the Seebeck coefficient, conductivity and power factor change at different temperatures. It can be seen that the conductivity decreases with increasing temperature. The modified PEDOT:PSS film exhibits obvious semi-metallic properties. Interestingly, the EG, etOH doping and EG post-treatment can simultaneously increase S and σ. Table 1 summarizes the carrier concentration (n) and mobility (μ) of PEDOT:PSS film and the films after three chemical treatments, the mobility and carrier concentration of the pristine PEDOT:PSS film are 0.23 $cm^2 V^{-1}s^{-1}$, $1.169x10^{20}$ cm^{-3}, respectively. Compared with the pristine PEDOT: PSS film, the mobility of the films treated with EG is significantly improved, which is 1.59 $cm^2V^{-1}s^{-1}$. After further treatment by using etOH, the Seebeck coefficient and conductivity of EG-sample are both improved, the carrier concentration decreases and the mobility increases after the incorporation of etOH, the specific value are 5.99 $cm^2V^{-1}s^{-1}$, 9.269×10^{20} cm^{-3} respectively. The change of the carrier concentration and mobility may be due to the energy filtering effect which can filter out the carrier with low energy and low mobility after doping etOH. Finally, the mobility and carrier concentration are 4.579 $cm^2V^{-1}s^{-1}$ and $2.016x10^{20}$ cm^{-3} respectively after immersion treatment. It has reached its maximum value. The concentration of four kinds of films are comparable, but the mobility is highly improved. We believe that the enhancement of mobility of PEDOT:PSS film have the main contribution on the improvement of electrical conductivity.

In order to unravel the mechanism of the thermoelectric properties improvement of PEDOT: PSS film after these treatments, we perform the vibrational spectra with Fourier transform infra-red (FTIR) spectroscopy, as shown in Figure 3 (a). The band at 1630 cm^{-1} is due to asymmetric stretching in the thiophene ring and the symmetric stretch vibration is found at 1385 cm^{-1} [23]. The peak at 1048 cm^{-1} is due to the C-O-C stretching vibration in ethylenedioxy. At the same time, C-S-C tensile deformation in the thiophene ring will cause peaks at 919 $cm^{-1}$and 829 cm^{-1}. See the table 2, infrared band assignments for pristine and treated PEDOT:PSS samples. In

View Article Online
DOI: 10.1039/C9TC06277G

addition, S=O and S-O stretching vibration in PSS will have characteristic peaks at 1193 cm^{-1}, 1164 cm^{-1} [23]. The weaker absorption bands may be related to the low concentration of PSS [24]. Besides, we monitor the peak position changes in the spectra of the thin films after three treatments and the pristine thin film. The results show that after adding EG, the hydroxyl peak at 3398 cm^{-1} blue shifts to 3436 cm^{-1}, indicating that intermolecular hydrogen bonding occurred [25], and C=C-O and C=C on the thiophene ring shifts slightly after treatment, which indicates that PEDOT and EG intermolecular hydrogen may be generated. We believe this may be the reason why EG can promote the phase separation of PEDOT and PSS.

Figure 3 (b) shows the X-ray diffraction (XRD) patterns of PEDOT: PSS films under different processing conditions. For the XRD pattern of the original sample, the diffraction peaks at low angles of 4.7° and 13.1° correspond to the lamellar stack of PEDOT in the (100) plane, while the other two peaks at 17.5° and 25. ° are attributed to PSS in the (010) plane amorphous stack. The observed results are in good agreement with the reported results [26]. After treatment with $(CH_2OH)_2$, the full width at half maxima (HWHM) of the diffraction peak at about 3.8° becomes narrower and shifts slightly to 4.2°, indicating that the crystallinity of the PEDOT molecule in the sample becomes better. After adding etOH and EG post-treatment, it is found that the diffraction peak of PSS becomes lower. Block, et al have found that ethanol and ethylene glycol post-treatment can combine the PSS molecules well to remove PSS [27]. Similarly, this effect makes the first two diffraction peaks shift to lower angles, and the HWHMs become narrower.

EPR measurements of Figure 3(c) are carried out to characterize the properties of polarons in different film [5, 21]. As the chemical doping process continues, the EPR signal of the film gradually decreases. There are conducting host molecules (PEDOT) and non-conducting PSS molecules in PEDOT: PSS solution. In the experiment, the doping of EG or et-OH and the de-doping by EG have different effects on each component of PEDOT: PSS solution. EG can form hydrogen bond with different PEDOT chains, which can reduce the distance

View Article Online
DOI: 10.1039/C9TC06277G

between PEDOT chain molecules, and thus reducing the loss of carrier jumping transmission between chains. As a monohydroxy molecule, et-OH can combine with sulfonic group in PSS to form a more hydrophilic salt than PEDOT chain, which can be removed after EG post-treatment. Proper removal of PSS is beneficial to increase the effective carrier concentration per unit volume. Briefly, these treatments adjust the thermoelectric properties of PEDOT: PSS at the molecular level. Whether reducing the distance between PEDOT chains or removing the non-conducting PSS, it is beneficial to increase the crystallinity of organic polymers and promote the molecular transformation from localized state to delocalized state. In conclusion, the decrease of EPR signal is due to the decrease of ions and the increase of delocalization state in the triple treated PEDOT: PSS films

In addition, in order to characterize whether PEDOT: PSS film is suitable as a light-to-heat conversion material, we performed UV absorption test on it, as shown in Figure 3 (d). In addition to visible light, PEDOT: PSS also has very good absorption in the near infrared region, which means that PEDOT: PSS uses solar energy very efficiently.

The addition of dopants can also affect the morphology of the film, leading to alternation of film thermoelectric properties. Figure 4 shows the AFM images before and after film processing. From the phase diagram of the original film, there is no obvious phase separation before processing. However, after processingit is obvious that the PEDOT chain and PSS chain are separated from each other, producing more fibrous interconnected conductive PEDOT chains. The degree of phase separation is related to the electrical conductivity. According to the literature [14, 28] , the bright region is conductive PEDOT, the dark region is insulating PSS in the Figure 4. Removaling PSS results in the stacking of PEDOT molecules which can promote the carrier transport.

3.2 Thermoelectric Properties of Ni

In order to achieve excellent thermoelectric performance based on PEDOT:PSS film, Ni is selected as n type legs in the thermoelectric modules. Figure 5 shows the thermoelectric properties of Ni in the horizontal direction

View Article Online
DOI: 10.1039/C9TC06277G

under different film thickness. The overall data shows that the Ni film is relatively stable as an n-type material, the Seebeck coefficient of Ni films with different thickness of 50, 100 and 150 nm are -18.66 μV/K, -17.61 μV/K, -18.42 μV/K, while the corresponding conductivity is 13080 S/cm, 14020 S/cm and 13640 S/cm at 50, 100 and 150 nm, respectively. To be economic and practicable, Ni with thickness of 150 nm was selected.

3.3 Utilization of module devices under photo-thermal condition

Motivated by the outstanding thermoelectric properties of both p-type and n-type materials, we propose a thermoelectric module with 6 pairs of n-p legs on glass substrate (Fig. 6 (a)). For the organic-inorganic fully integrated module device, we have illustrated the effect of the module device on photothermal conversion process [29-30]. Before measuring the thermoelectric performance of the module device under light, we apply thermal insulation paint to the cold end of the module device to prevent heat diffusing from the hot end to the cold end, thereby forming a large temperature difference between the cold and hot ends. With the increase of illumination time, both the temperature gradient (ΔT) and the hot side temperature (T_{hot}) increase, the highest ΔT can reach 11.8 K (see the table 3). In details, Fig. 6 (a) exhibits the open circuit voltage and short circuit current of the device using sunlight as heat source. With the increase of T_{hot} and ΔT, the Seebeck voltage and short circuit current increase gradually. ΔT of 11.8 K is the maximum temperature gradient originating from the solar thermal radiation when the temperature at the hot side is 328 K, the Seebeck voltage attain 3.17 mV and the short circuit current reach 8.4 μA. The connection of PEDOT:PSS and Ni shows an accumulation of output thermovoltage. If a better light absorption concentrator is used, the device temperature will continue to rise, and the ΔT will further increase. Therefore, a simulation experiment of the device thermoelectric conversion effect using a heater as a heat source (Fig. 6 (b)) is proposed. It can be seen that the temperature of the device increases with increasing the heating temperature, the device temperature can vary from 328 K to 348 K. With the increasement of ΔT, the voltage and short-circuit current of the device continuely increase. When the maximum temperature up to 348 K, the Seebeck

View Article Online
DOI: 10.1039/C9TC06277G

voltage can reach to 5.06 mV and the short-circuit current is 10.6 uA, comparing with Figure 6 (a), the Seebeck voltage and short-circuit current fluctuate more greatly. It indicates that photothermal conversion method can enhance the stability of the power output process of the module.

The power output of the module with different external resistance is measured at the above temperature (Fig.6 (c)).The power output is calculated through $P_{max} = U^2/(4R)$, where U is the experimental voltage and R is the external resistance [31-32]. It should be noted that the real part of the output power is the result of photothermal conversion, and the virtual part is the external heat source. The results show that the output power magnifies with the increase of T_{hot} and ΔT . Specifically, when the high temperature terminal is 328 K, the power output of the module device is 9.8 nw. However, the conventional power output test shows the maximum power output of the module device is 23 nw under 348 K. These results also reveal the application prospect of the module device in the photothermal utilization. Furthermore, we have mesuared the air stability of thermoelectric modules. The module with the power output of 11 nW is storaged in air with the humidity of 65%. After 100 hours, the module shows a power output of 11 nW, which is similar to the original value without degradation. It indicates the module shows good air stability.

4. Conclusion

In summary, we have developed a thermoelectric generator with p-legs of the high-performance PEDOT :PSS and n-legs of Ni to improve the utilization of solar energy photothermal conversion, According to the order of $(CH_2OH)_2$, C2H5OH doping and $(CH_2OH)_2$ post-treatment, we modify the pristine PEDOT: PSS material, and obtain the film with the highest PF of 330.597 μWm^{-1} at room temperature. At the molecular level, these treatments improve the crystalline properties of organic polymer molecules, optimize the carrier transport path, and finally obtain high-performance films. On the basis of the above work. We make this modular device to explore the photothermal conversion process of thermoelectric generators. Moreover, the maximum power output of the device

View Article Online
DOI: 10.1039/C9TC06277G

is 9.8 nW in the process of photothermal conversion .The work of this paper provides an experimental support for development of the solar energy photothermal conversion in the field of thermoelectric materials and devices.

Acknowledgements

The authors gratefully acknowledge financial support from the Fundamental Research Funds for the Central Universities in Huazhong University of Science and Technology (Grant No. 2016YXMS033), the Double first-class research funding with independent intellectual property of ICARE (Grant No. 3011187028), and supported by the Fundamental Research Funds for the Central Universities, HUST（Grant No. 2017KFXKJC001）, and supported by the Hubei natural science foundation (Grant No. 2019CFB463) .The authors would like to thank the Analytical and Testing Center of Huazhong University of Science and Technology for providing the facilities to conduct the characterization.

View Article Online
DOI: 10.1039/C9TC06277G

References

1. Chen, C.; Kuang, Y.; Hu, L., Challenges and opportunities for solar evaporation. *Joule* **2019**.
2. NREL，National Renewable Energy Laboratory，https://baijiahao.baidu.com/s?id=1641007748124043683 &wfr=spider&for=pc.
3. Leung, W. W.; Savory, C. N.; Palgrave, R. G.; Scanlon, D. O., An experimental and theoretical study into NaSbS 2 as an emerging solar absorber. *Journal of Materials Chemistry C* **2019,** *7* (7), 2059-2067.
4. Kraemer, D.; Poudel, B.; Feng, H.-P.; Caylor, J. C.; Yu, B.; Yan, X.; Ma, Y.; Wang, X.; Wang, D.; Muto, A., High-performance flat-panel solar thermoelectric generators with high thermal concentration. *Nature materials* **2011,** *10* (7), 532.
5. Peng, L.; Liu, Z., Enhancing thermoelectric properties by using a surface polarization effect based on PEDOT: PSS thin films. *Journal of Materials Chemistry C* **2019,** *7* (20), 6120-6128.
6. Meng, Q.; Cai, K.; Du, Y.; Chen, L., Preparation and thermoelectric properties of SWCNT/PEDOT: PSS coated tellurium nanorod composite films. *Journal of Alloys and Compounds* **2019,** *778*, 163-169.
7. Kim, J.-Y.; Lee, W.; Kang, Y. H.; Cho, S. Y.; Jang, K.-S., Wet-spinning and post-treatment of CNT/PEDOT: PSS composites for use in organic fiber-based thermoelectric generators. *Carbon* **2018,** *133*, 293-299.
8. Bae, E. J.; Kang, Y. H.; Jang, K.-S.; Lee, C.; Cho, S. Y., Solution synthesis of telluride-based nano-barbell structures coated with PEDOT: PSS for spray-printed thermoelectric generators. *Nanoscale* **2016,** *8* (21), 10885-10890.
9. Wei, Q.; Mukaida, M.; Kirihara, K.; Naitoh, Y.; Ishida, T., Recent progress on PEDOT-based thermoelectric materials. *Materials* **2015,** *8* (2), 732-750.
10. Bender, K.; Gogu, E.; Hennig, I.; Schweitzer, D.; Müenstedt, H., Electric conductivity and thermoelectric power of various polypyrroles. *Synthetic Metals* **1987,** *18* (1-3), 85-88.
11. Taylor, P. S.; Korugic-Karasz, L.; Wilusz, E.; Lahti, P. M.; Karasz, F. E., Thermoelectric studies of oligophenylenevinylene segmented block copolymers and their blends with MEH-PPV. *Synthetic Metals* **2013,** *185*, 109-114.
12. Kalagi, S. S.; Patil, P. S., Secondary electrochemical doping level effects on polaron and bipolaron bands evolution and interband transition energy from absorbance spectra of PEDOT: PSS thin films. *Synthetic Metals* **2016,** *220*, 661-666.

13. Wei, Q.; Mukaida, M.; Naitoh, Y.; Ishida, T., Morphological change and mobility enhancement in PEDOT: PSS by adding co-solvents. *Advanced materials* **2013,** *25* (20), 2831-2836.

14. Luo, J.; Billep, D.; Waechtler, T.; Otto, T.; Toader, M.; Gordan, O.; Sheremet, E.; Martin, J.; Hietschold, M.; Zahn, D. R., Enhancement of the thermoelectric properties of PEDOT: PSS thin films by post-treatment. *Journal of Materials Chemistry A* **2013,** *1* (26), 7576-7583.

15. Fan, Z.; Li, P.; Du, D.; Ouyang, J., Significantly Enhanced Thermoelectric Properties of PEDOT: PSS Films through Sequential Post-Treatments with Common Acids and Bases. *Advanced Energy Materials* **2017,** *7* (8), 1602116.

16. Kim, G. H.; Shao, L.; Zhang, K.; Pipe, K. P., Engineered doping of organic semiconductors for enhanced thermoelectric efficiency. *Nature materials* **2013,** *12* (8), 719.

17. Wang, S.; Xu, J.; Wang, W.; Wang, G.-J. N.; Rastak, R.; Molina-Lopez, F.; Chung, J. W.; Niu, S.; Feig, V. R.; Lopez, J., Skin electronics from scalable fabrication of an intrinsically stretchable transistor array. *Nature* **2018,** *555* (7694), 83.

18. Baranowski, L. L.; Snyder, G. J.; Toberer, E. S., Concentrated solar thermoelectric generators. *Energy & Environmental Science* **2012,** *5* (10), 9055-9067.

19. Olsen, M.; Warren, E.; Parilla, P.; Toberer, E.; Kennedy, C.; Snyder, G.; Firdosy, S.; Nesmith, B.; Zakutayev, A.; Goodrich, A., A high-temperature, high-efficiency solar thermoelectric generator prototype. *Energy Procedia* **2014,** *49*, 1460-1469.

20. Hua, Q.; Sun, J.; Liu, H.; Bao, R.; Yu, R.; Zhai, J.; Pan, C.; Wang, Z. L., Skin-inspired highly stretchable and conformable matrix networks for multifunctional sensing. *Nature communications* **2018,** *9* (1), 244.

21. Kim, D.-H.; Han, S. In *Evaluation of effects on the performance of thermoelectric generators using solar energy*, Proceedings of KSES 2013 spring conference, 2013; pp 41-46.

22. Cho, Y.; Park, Y.; Yang, Y., An experimental study of the solar thermoelectric generation system. *Solar Energy* **1998,** *18* (3), 113-118.

23. Mitraka, E.; Jafari, M. J.; Vagin, M.; Liu, X.; Fahlman, M.; Ederth, T.; Berggren, M.; Jonsson, M.; Crispin, X., Oxygen-induced doping on reduced PEDOT. *Journal of Materials Chemistry A* **2017,** *5* (9), 4404-4412.

24. Khan, Z. U.; Bubnova, O.; Jafari, M. J.; Brooke, R.; Liu, X.; Gabrielsson, R.; Ederth, T.; Evans, D. R.; Andreasen, J. W.; Fahlman, M., Acido-basic control of the thermoelectric properties of poly (3, 4-ethylenedioxythiophene) tosylate (PEDOT-Tos) thin films. *Journal of Materials Chemistry C* **2015,** *3* (40), 10616-10623.

25. Espinosa, E.; Molins, E.; Lecomte, C., Hydrogen bond strengths revealed by topological analyses of experimentally observed electron densities. *Chemical Physics Letters* **1998,** *285* (3-4), 170-173.

26. Xu, S.; Hong, M.; Shi, X.-L.; Wang, Y.; Ge, L.; Bai, Y.; Wang, L.; Dargusch, M.; Zou, J.; Chen, Z.-G., High-performance PEDOT: PSS flexible thermoelectric materials and their devices by triple post-treatments. *Chemistry of Materials* **2019,** *31* (14), 5238-5244.

27. Maeda, R.; Kawakami, H.; Shinohara, Y.; Kanazawa, I.; Mitsuishi, M., Thermoelectric properties of PEDOT/PSS films prepared by a Gel-film formation process. *Materials Letters* **2019,** *251*, 169-171.

28. Cui, M.; Song, Z.; Wu, Y.; Guo, B.; Fan, X.; Luo, X., A highly sensitive biosensor for tumor maker alpha fetoprotein based on poly (ethylene glycol) doped conducting polymer PEDOT. *Biosensors and Bioelectronics* **2016,** *79*, 736-741.

29. Zhao, L.; Yang, Z.; Cao, Q.; Yang, L.; Zhang, X.; Jia, J.; Sang, Y.; Wu, H.-J.; Zhou, W.; Liu, H., An earth-abundant and multifunctional Ni nanosheets array as electrocatalysts and heat absorption layer integrated thermoelectric device for overall water splitting. *Nano energy* **2019,** *56*, 563-570.

30. Zhu, L.; Ding, T.; Gao, M.; Peh, C. K. N.; Ho, G. W., Shape Conformal and Thermal Insulative Organic Solar Absorber Sponge for Photothermal Water Evaporation and Thermoelectric Power Generation. *Advanced Energy Materials* **2019,** *9* (22), 1900250.

31. Park, S.-J.; Gazzola, M.; Park, K. S.; Park, S.; Di Santo, V.; Blevins, E. L.; Lind, J. U.; Campbell, P. H.; Dauth, S.; Capulli, A. K., Phototactic guidance of a tissue-engineered soft-robotic ray. *Science* **2016,** *353* (6295), 158-162.

32. Sun, Y.; Sheng, P.; Di, C.; Jiao, F.; Xu, W.; Qiu, D.; Zhu, D., Organic Thermoelectric Materials and Devices Based on p-and n-Type Poly (metal 1, 1, 2, 2-ethenetetrathiolate) s. *Advanced Materials* **2012,** *24* (7), 932-937.

View Article Online
DOI: 10.1039/C9TC06277G

Figure and Table Captions

Table 1. Carrier concentration and mobility of three treated samples.

Table 2. Infrared band assignments for pristine and treated PEDOT:PSS samples.

Table 3. The surface temperature of PEDOT:PSS film under sunlight illuminate.

Figure 1 (a) PEDOT:PSS molecule structure, (b) P-type and N-type thermoelectric generator structure.

Figure 2 (a) Conductivity, Seebeck coefficient and Power factor diagram of PEDOT: PSS treated with EG, EG-etOH, EG-etOH-EG, respectively, are measured at 273 K. (b) Thermoelectric properties of PEDOT: PSS treated with EG-etOH-EG at different temperatures.

Figure 3 (a) The FTIR spectra of pristine and treated PEDOT:PSS films. The arrows indicate peak position changes from the quinoid (pristine) to the benzoid structures. Further details of the labeled bands can be found in Table 2. (b) The results of XRD for PEDOT:PSS films with different treating conditions (c) The EPR signal of PEDOT:PSS, (d) The absorption spectrum of PEDOT:PSS films under different treatments.

Figure 4 AFM images of PEDOT films under different chemical treatments (a) original, (b) EG, (c) EG-etOH, (d) EG-etOH-EG, (e),(f), (g), (h) are the corresponding phase diagrams. All images are 500nm×500nm

Figure 5 The Seebeck coefficient, electrical conductivity, and Power Factor value of Ni films with 50,100,150 nm thickness.

Figure 6 Output thermoelectric parameters of P-type and N-type thermoelectric modules (PEDOT: PSS+Ni). (a) Using sunlight as a heat source, Seebeck voltage and short-circuit current related to temperature and temperature difference. (b) Using a hot stage as a heat source, Seebeck voltage and short-circuit current related to temperature and temperature difference. (c) Power output stability of the module operating at T_{hot}=318 K. (d) Power output under different temperatures.

View Article Online
DOI: 10.1039/C9TC06277G

Table 1. Carrier concentration and mobility of three treated samples.

parameter	Pristine	EG	EG-etOH	EG-etOH-EG
n (10^{20} cm^{-3})	1.169	2.132	9.269	2.016
μ ($cm^2V^{-1}s^{-1}$)	0.23	1.59	5.99	4.58

Table 2. Infrared band assignments for pristine and treated PEDOT:PSS samples.

Assignments	Pristine(cm^{-1})	$(CH_2OH)_2$	$(CH_2OH)_2$-C_2H_5OH	$(CH_2OH)_2$-C_2H_5OH-$(CH_2OH)_2$	Shift(cm^{-1})	References
$\nu(COC)$	1054	1047	1047	1047	7	23
$\nu(CSC)$	835	838	829	838	3	23
$\nu(O-C=C)$	1309	1388	1388	1388	79	24
$\nu(C=C)$	1635	1633	1633	1633	2	24
$\nu(C-C)$	2921	2922	2922	2922	1	23
$\nu(O-H)$	3411	3488	3488	3488	38	25

Table3. PEDOT:PSS thin film surface temperature under sunlight illuminate.

T_{hot} (K)	303	308	313	318	323	328
△T(K)	3.7	6.2	8.0	9.3	10.4	11.8

View Article Online
DOI: 10.1039/C9TC06277G

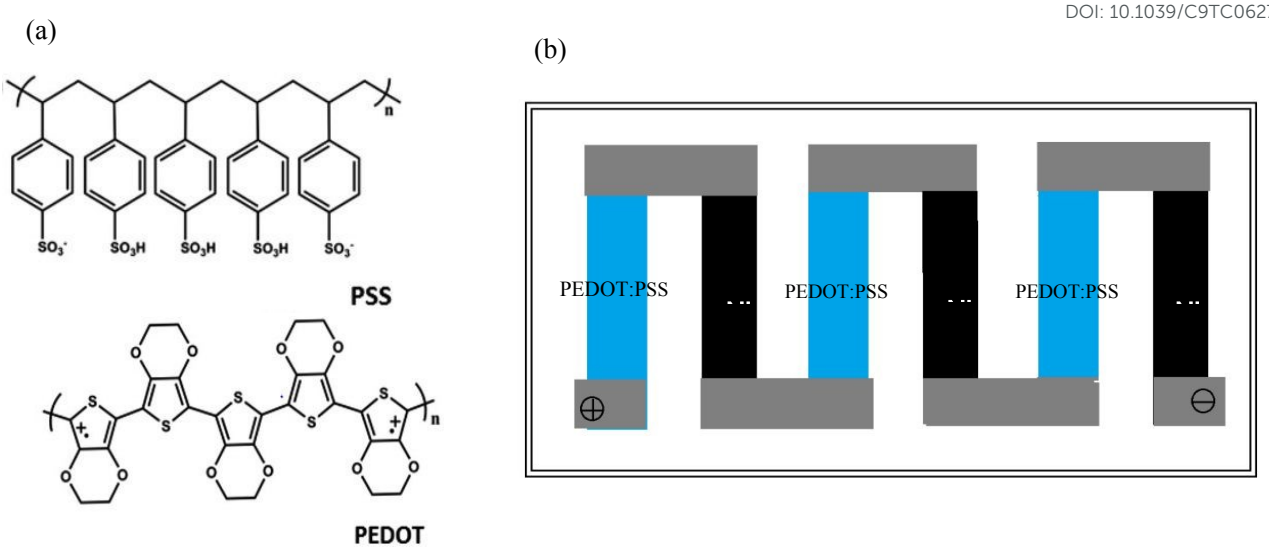

Figure 1. (a) PEDOT:PSS molecule structure, (b) P-type and N-type thermoelectric generator structure.

View Article Online
DOI: 10.1039/C9TC06277G

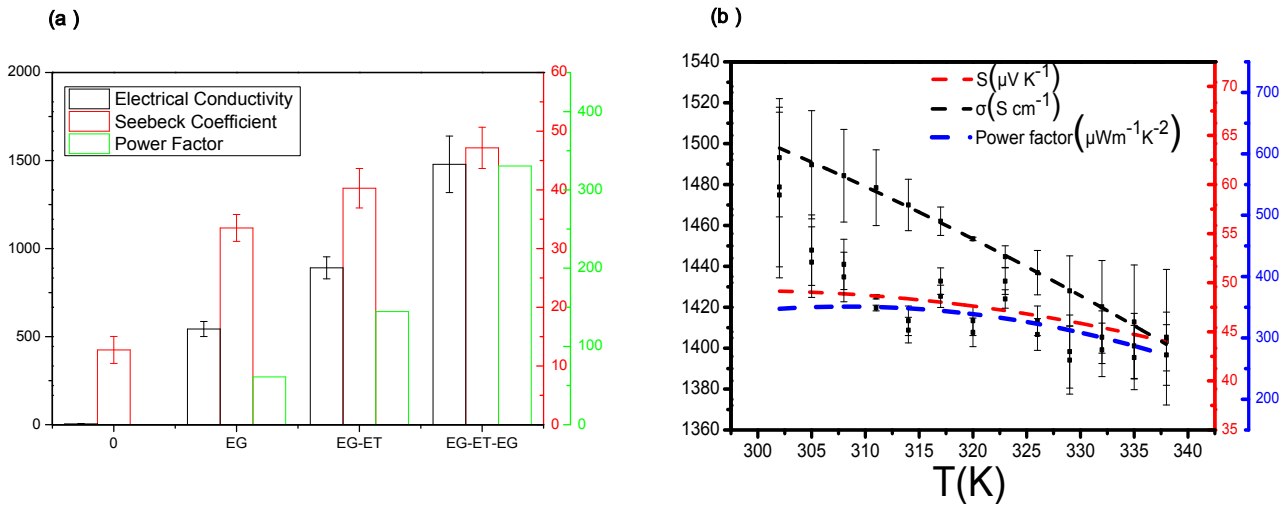

Figure 2. (a) Conductivity, Seebeck coefficient and Power factor diagram of PEDOT: PSS treated with EG, EG-etOH, EG-etOH-EG, respectively, are measured at 273 K. (b) Thermoelectric properties of PEDOT: PSS treated with EG-etOH-EG at different temperatures.

View Article Online
DOI: 10.1039/C9TC06277G

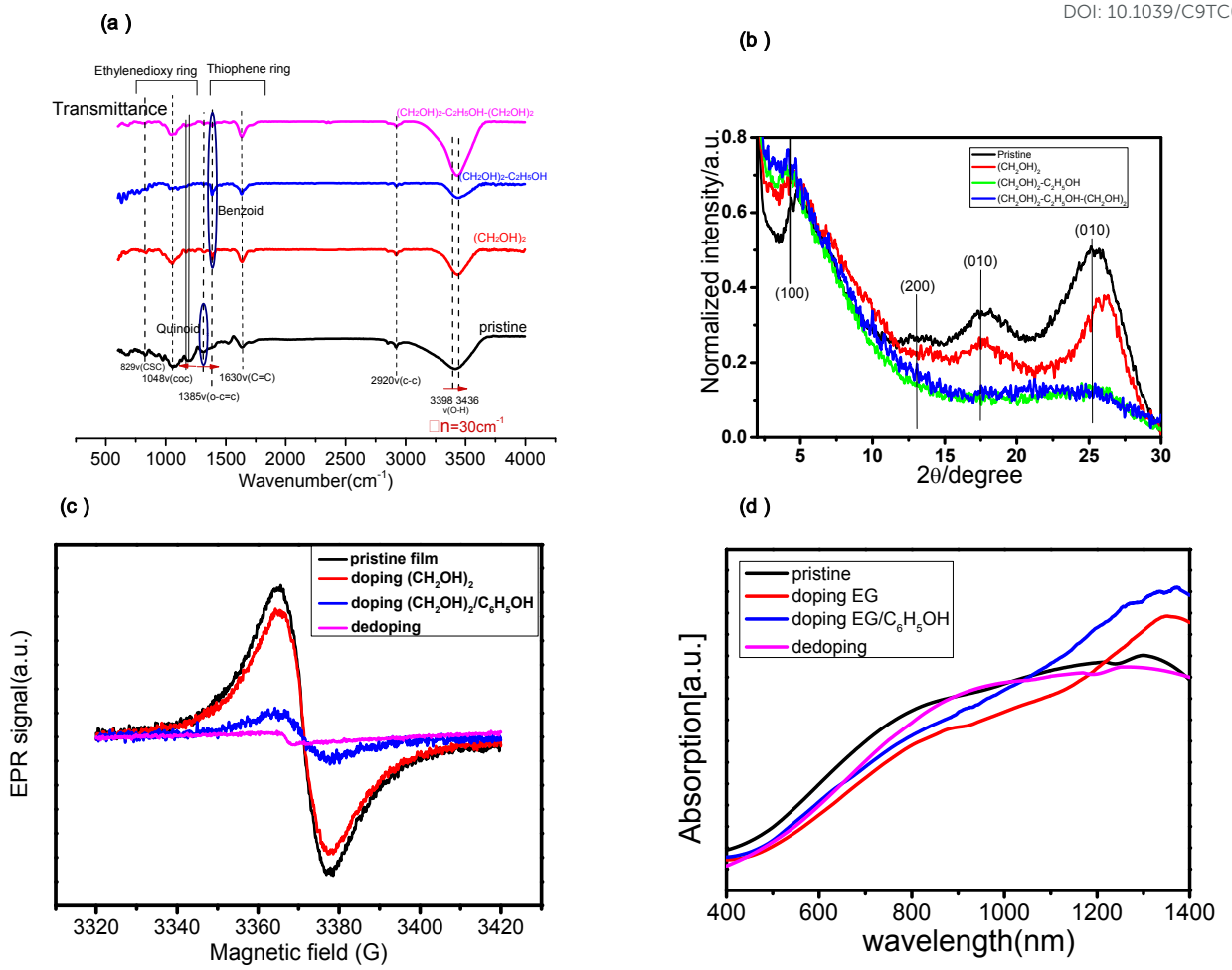

Figure 3. (a) The FTIR spectra of pristine and treated PEDOT:PSS films. The arrows indicate peak position changes from the quinoid (pristine) to the benzoid structures. Further details of the labeled bands can be found in Table 2. (b) The results of XRD for PEDOT:PSS films with different treating conditions (c) The EPR signal of PEDOT:PSS, (d) The absorption spectrum of PEDOT:PSS films under different treatments.

View Article Online
DOI: 10.1039/C9TC06277G

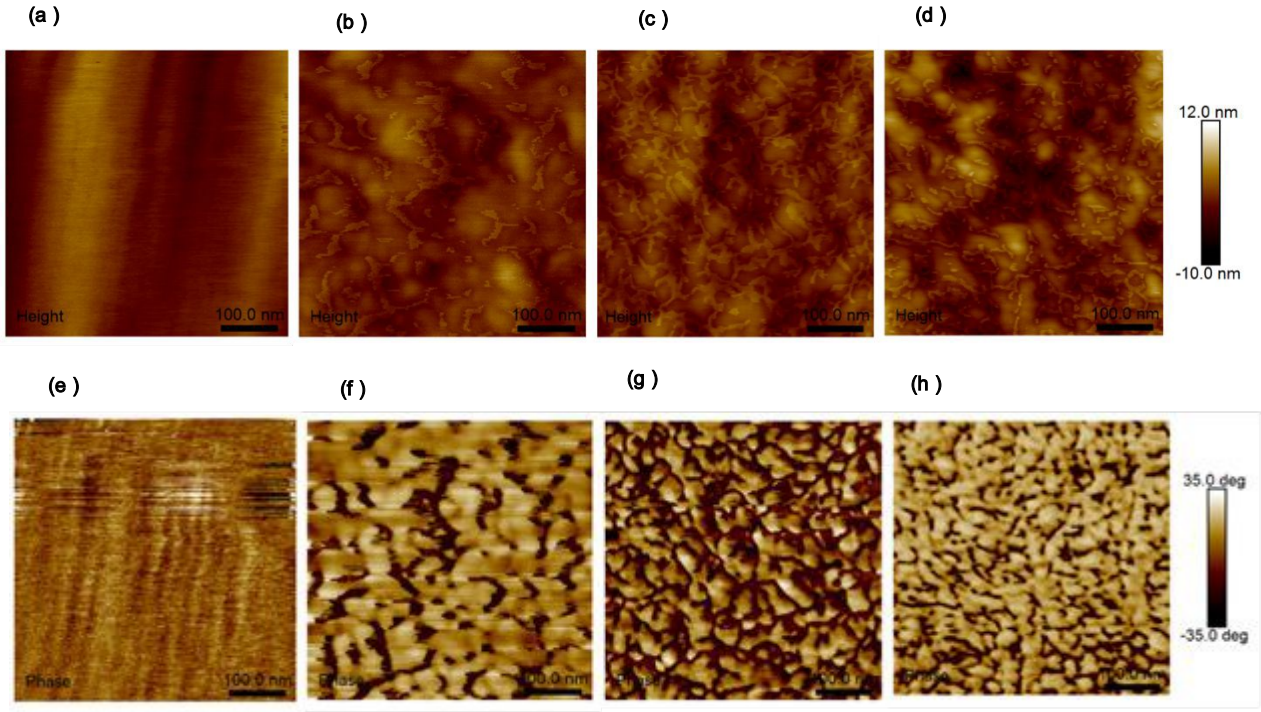

Figure 4 AFM of PEDOT under different chemical treatments (a), (b), (c), (d) original, EG, EG-etOH, EG-etOH-EG After the treated film, (e),(f), (g), (h) is the corresponding phase diagram. All images are 500 nm×500 nm.

View Article Online
DOI: 10.1039/C9TC06277G

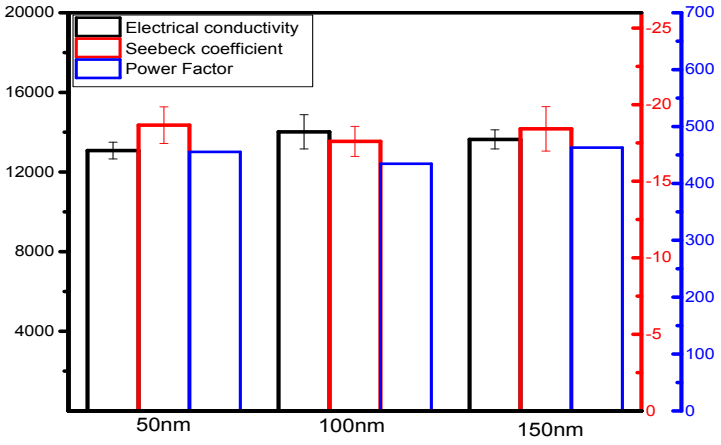

Figure 5 Ni thermoelectric properties of Seebeck coefficient, electrical conductivity, and Power Factor value with the 50,100,150 nm thickness .

View Article Online
DOI: 10.1039/C9TC06277G

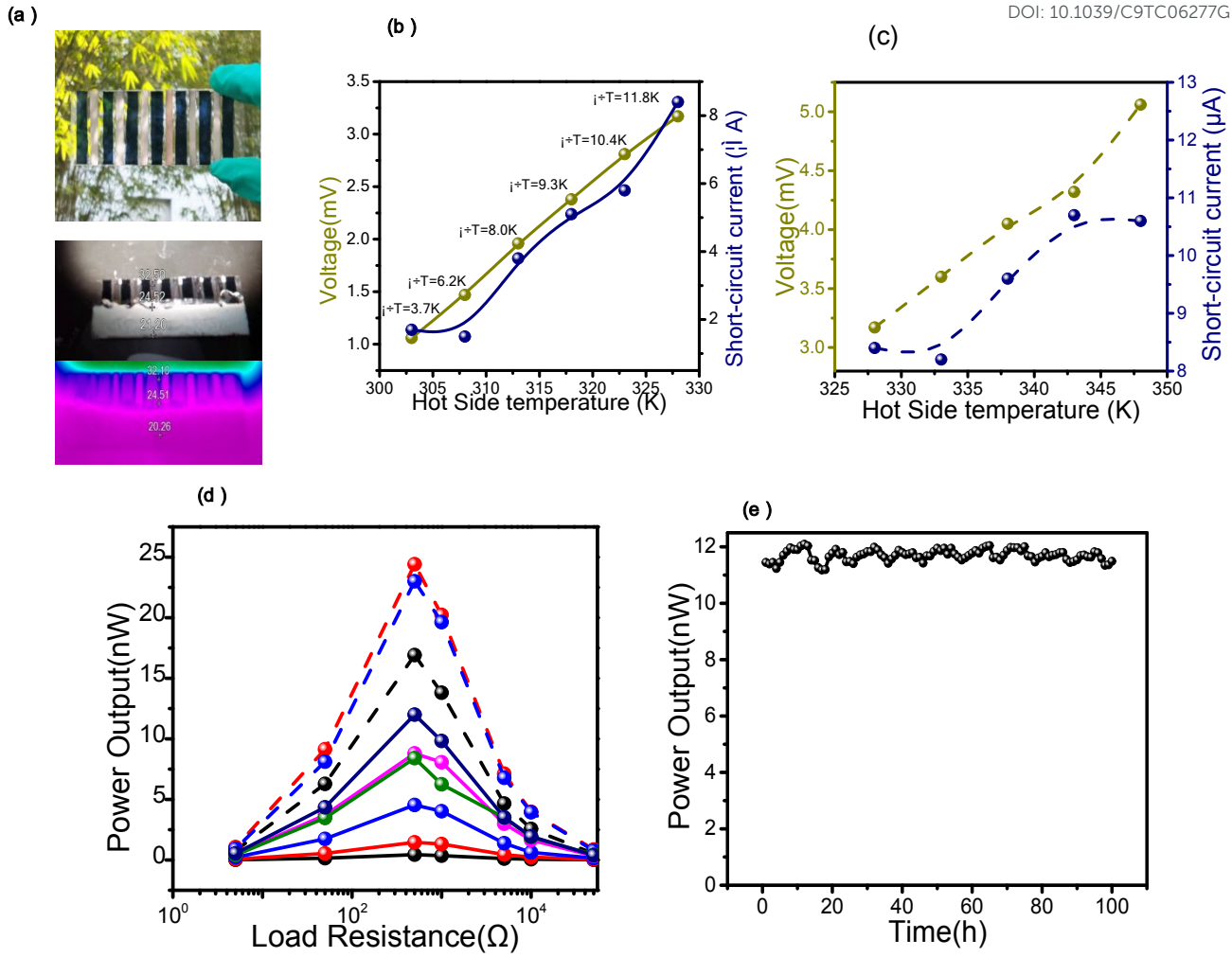

Figure 6. Output thermoelectric parameters of P-type and N-type thermoelectric modules (PEDOT: PSS+Ni).(a) Using sunlight as a heat source, Seebeck voltage and short-circuit current related to temperature and temperature difference.(b) Using a hot stage as a heat source, Seebeck voltage and short-circuit current related to temperature and temperature difference.(c) Power output stability of the module operating with T_{hot}=318K.(d)different temperature power output. Infrared images of the module under operating condition with sunlight irradiation

View Article Online
DOI: 10.1039/C9TC06277G

Highlights

1. We used an inexpensive and effective way to improve the thermoelectric properties of PEDOT:PSS.
2. We obtained the PEDOT:PSS thermoelectric film material with the highest power factor up to 330.597 μWm^{-1}.
3. Overall data shows that the Ni film is relatively stable as an n-type material, Ni as a n-leg in the thermoelectric module.
4. We fabricated thermoelectric generator to explore the photothermal conversion process of solar energy.

View Article Online
DOI: 10.1039/C9TC06277G

ToC Figure